

# EUROPEAN SYNCHROTRON RADIATION FACILITY

ESRF User Office

BP 220, F-38043 GRENOBLE CEDEX, France

Delivery address: 6 rue Jules Horowitz, 38043 GRENOBLE, France

Tel: +33 (0)4 7688 2552; fax: +33 (0)4 7688 2020; email: [useroff@esrf.fr](mailto:useroff@esrf.fr); web:

<http://www.esrf.fr>



---

## **Mechanism of birnessite during electrodeposition and identification of solid precursors by in-situ grazing-incidence X-ray diffraction.**

S. Peulon, M. Ndjeri, A. Chaussé

Laboratoire Analyse et Modélisation pour la Biologie et l'Environnement (LAMBE)

UMR 8587 (CNRS-CEA-Université d'Evry) Bd François Mitterrand 91025 Evry Cedex

M. L. Schlegel,

Laboratoire de Réactivité des Surfaces et des Interfaces, Bât 391, CEA Saclay

### **I - Context**

The main goal of these experiments was to test the possibility to characterise thin layers of various material(s) during electrodeposition and oxidation and/or reduction by XRD using synchrotron measurements (ESRF- Grenoble-BM32). For that, a special electrochemical cell was developed in our laboratory, which was already validated for efficient electrochemical measurements. We have chosen to test this special electrochemical cell by studying the electrodeposition of thin layers of birnessite, and their electrochemical reduction.

Birnessite (nominally  $Mn_7O_{13} \cdot H_2O$ ) is a major Mn mineral phase in many soils [1]. These minerals have a layered structure formed by  $MnO_6$  octahedra sharing edges. Birnessite compounds often deviate from stoichiometry due to the substitution of some Mn(IV) by Mn(III) or Mn(II), with hydrated alkaline cations ( $Na^+$ ,  $K^+$ ,  $Ca^{2+}$  ...) in the interlayer that compensate the layer negative charge [2,3]. These alkaline cations, located in the interlayers, can be exchanged with other cations, such as  $Pb^{2+}$ ,  $Cu^{2+}$ ,  $Co^{2+}$ ,  $Cd^{2+}$  and  $Zn^{2+}$  [4]. Moreover, birnessite-type compounds readily participate in oxidation-reduction reactions via a surface mechanism (oxidation of Se(IV) to Se(VI) [5], Cr(III) to Cr(VI) [6], As(III) to As(V) [7]...). Because of these unique sorption and redox properties, birnessite minerals are under scrutiny as major scavengers of trace metals in the environment. They also attract considerable

scientific interest as inexpensive and non-toxic materials for hazardous waste remediation [8-10], rechargeable battery technology [11-13] or chemical sensors [14,15].

Very few studies report the synthesis of birnessite as thin films by electrochemical synthetic procedures [16,17], however, layers directly deposited on current collectors present very attractive potential applications regarding redox transformations. Previously, we reported successful electrodeposition of thin layers of various compounds onto SnO<sub>2</sub> [18,19] and birnessite in particular, in soft conditions (without deaeration) [20].

Moreover, from a survey of the literature, one notes that the nature of birnessite depends greatly on the pH of the solution and that its formation is a very complex process [21,22]. That is why, we focussed this study on the influence of medium on the electrodeposition of thin layers of birnessite (nature of cation: Na<sup>+</sup>, K<sup>+</sup>; pH). We tested also the possibility to study the redox behaviour of these thin layers in various conditions, in particular, in absence or presence of Mn(II) ions in solution.

## II - Experimental conditions

The electrochemical cell containing three electrodes was specially developed for synchrotron measurements in our laboratory (Fig.1). The reference electrode was a microelectrode Ag/AgCl home made ([NaCl] = 0.1 M,  $E_{\text{ref}} = 0.29 \text{ V}/E_{\text{SH}}$ ). All potential values cited in the text are referred to this reference electrode. The counter electrode was a film of kapton doped with carbon (Goodfellows, Kapton XC, 370  $\Omega/\text{cm}^2$ ). The working electrode was a glass plate covered with tin dioxide (SOLEMS, 120  $\Omega/\text{cm}^2$ , 15 X 60 mm) used as received. The plate was cut and the surface in contact with electrolyte was equal to  $S = 3 \text{ cm}^2$  (15 X 20 mm)

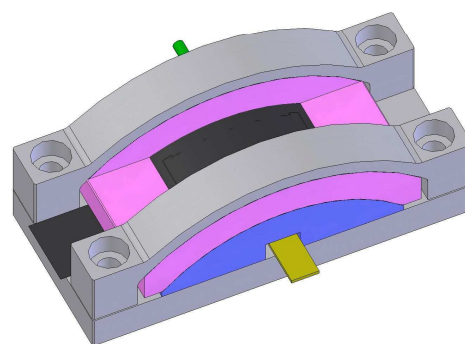


Fig. 1: Overview of the electrochemical cell for *in situ* surface electrochemistry coupled with X-ray diffraction.

The volume of the cell was evaluated at around 2 mL. The solution was introduced inside the cell by using a piloted micropump (mp5 and extended micropump control, Bartels, microtechnik) and circulated in continuous during electrochemical measurements. The best parameters to obtain reproducible measurements were:

- Signal form: Sine
- Frequency range: 20 Hz
- Amplitude range  $V = 250$  Vpp

In these conditions, the rate of flow was estimated at around 1.25 mL/mn.

All electrochemical measurements were performed at room temperature using a microautolab potentiostat / galvanostat system (Eco Chemie) controlled by a Dell Computer using the GPES software package (version 4.9). The crystal structures were determined in-situ during electrochemical measurements using synchrotron measurements (ESRF- Grenoble – BM32). The measurements were made at 20 kV ( $\lambda_{\text{ESRF}} = 0.6192 \text{ \AA}$ ). The ex-situ measurements were made in the cell in the air after only that the sample was rinsed by circulation of milli-Q water inside the cell (10 mn) before that the film of kapton was removed (same geometry).

Reagents,  $\text{MnSO}_4$ ,  $\text{H}_2\text{O}$  (ACS Reagent Aldrich),  $\text{Na}_2\text{SO}_4 \cdot 10\text{H}_2\text{O}$  (ACS Reagent Sigma Aldrich),  $\text{K}_2\text{SO}_4 \cdot 10\text{H}_2\text{O}$  (99 % ACS Reagent Sigma Aldrich),  $\text{H}_2\text{SO}_4$  (1 mol.L<sup>-1</sup>, Standard solution, Riedel-de-Haën), were used without further purification. The solutions ( $\text{Na}_2\text{SO}_4$  0.4 mol.L<sup>-1</sup> or  $\text{K}_2\text{SO}_4$  0.4 mol.L<sup>-1</sup>;  $[\text{MnSO}_4] = 1.6 \cdot 10^{-3}$  mol.L<sup>-1</sup>) were prepared just before experiments with 18 M $\Omega$ .cm Milli-Q water. The initial pH was measured with a combined pH electrode (WTW SenTix 97/T; pH-meter WTW - Multiline P4), and adjusted by addition of  $\text{H}_2\text{SO}_4$  (0.1 mol.L<sup>-1</sup>) if necessary. For all experiments, the solutions were used without deaeration.

### III – Electrodeposition of thin layers of birnessite in presence of $\text{Na}^+$ .

#### III – 1 Preliminary measurement

We determined the main patterns of the substrate ( $\text{SnO}_2$ ) alone in the air (Fig. 2A), and when the electrolyte solution ( $\text{Na}_2\text{SO}_4$  0.4 M) was in circulation inside the cell, (Fig. 2B), to evaluate the impact of aqueous solution on the quality of the signals.

Fig. 2A

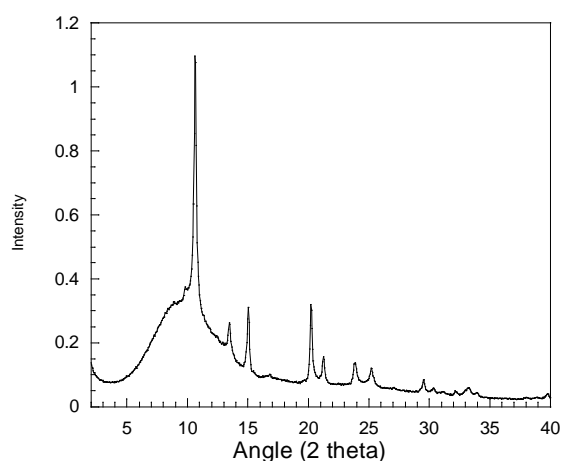
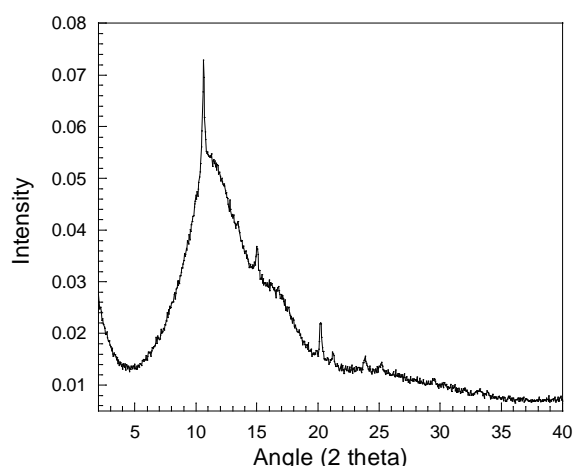


Fig. 2B



In the air, the main patterns of SnO<sub>2</sub> (JCPDS card 41-1445) were found with significant intensities, Table 1. The substrate must have a preferential orientation because the peak at 13.47 ° has a smaller intensity than in theory. As expected, the presence of aqueous solution in the electrochemical cell (thin layer around 1 mm thickness) degrades the signal, but the main peaks are always present proving that it is possible to determine the structure of crystallised compounds, Table 1.

SnO <sub>2</sub> (cassiterite) JCPDS card 14-1445 (°) - ( $\lambda_{\text{ESRF}} = 0.6192 \text{ \AA}$ )	Experimental measurements	
	In the air (°) - ( $\lambda_{\text{ESRF}} = 0.6192 \text{ \AA}$ )	In Na <sub>2</sub> SO <sub>4</sub> (°) - ( $\lambda_{\text{ESRF}} = 0.6192 \text{ \AA}$ )
10.61 (100 %)	<b>10.61</b>	<b>10.60</b>
13.47 (75 %)	13.47	-
15.08 (21 %)	<b>15.08</b>	<b>15.00</b>
20.13 (57 %)	<b>20.17</b>	<b>20.19</b>
21.20 (14 %)	21.25	21.22 (vw)
23.83 (11 %)	23.83	23.88 (vw)
25.19 (14 %)	25.25	25.20 (vw)

vw: very weak

Table 1

### *III – 2 Electrodeposition of thin layer of birnessite: determination of the intermediary compound in standard conditions (Na<sub>2</sub>SO<sub>4</sub>, pH<sub>initial</sub> = 5.3)*

Thin layers of birnessite were electrodeposited in standard conditions ([MnSO<sub>4</sub>] = 1.6 10<sup>-3</sup> M in a Na<sub>2</sub>SO<sub>4</sub> 0.4 M solution) by chronoamperometry (imposition of a constant potential: E = 0.9 V) (Sample 2) [20]. The final amount of electricity (Q<sub>f</sub>) is equal to 1.88 C after 10600 seconds and the value of pH<sub>final</sub> = 4.55. As reported previously, we observed a systematic decrease of pH. This evolution is in accordance with a significant oxidation of Mn(II) ions and a liberation of protons [20]. Fig. 3A shows I = f(t) and Q = f(t) (insert) during electrodeposition. The charge Q increases linearly with time suggesting that the electro-oxidation of Mn(II) ions is a homogeneous process due to a good electronic conduction of the deposited film. During electrodeposition, systematic XRD measurements were recorded at

constant times (2 – 22 °, step: 0.05 ° - 2 s/step, 800 s for each scan); only half of scans was represented on Fig. 3B.

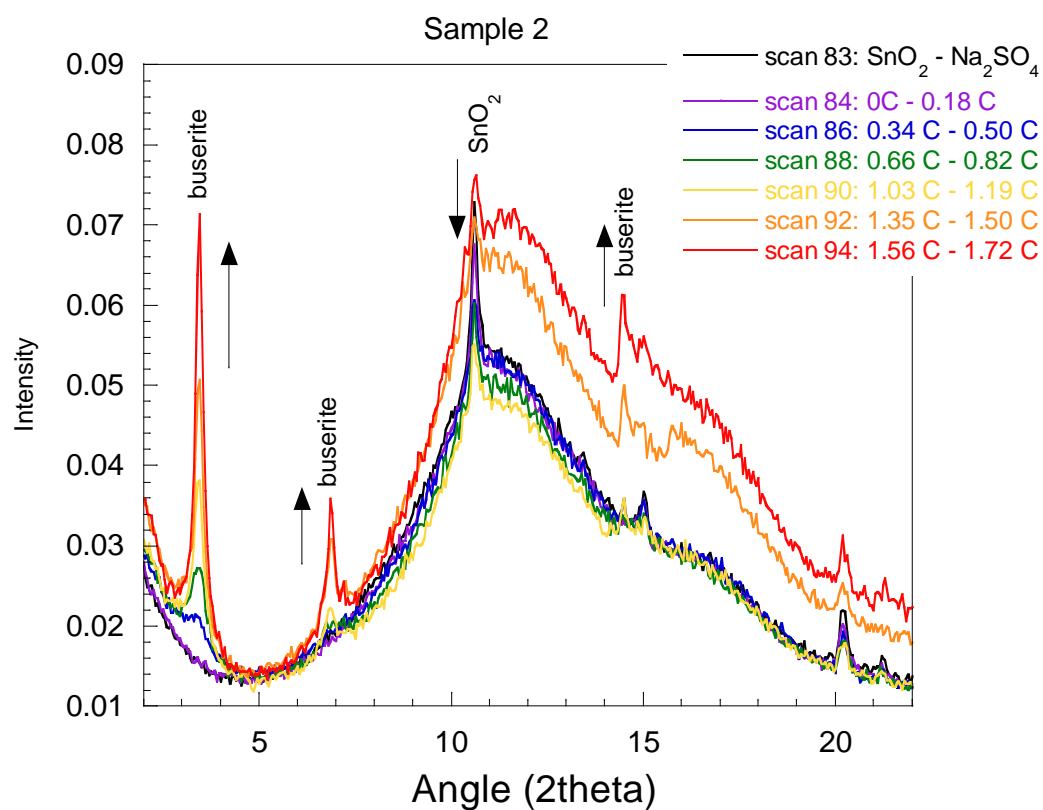
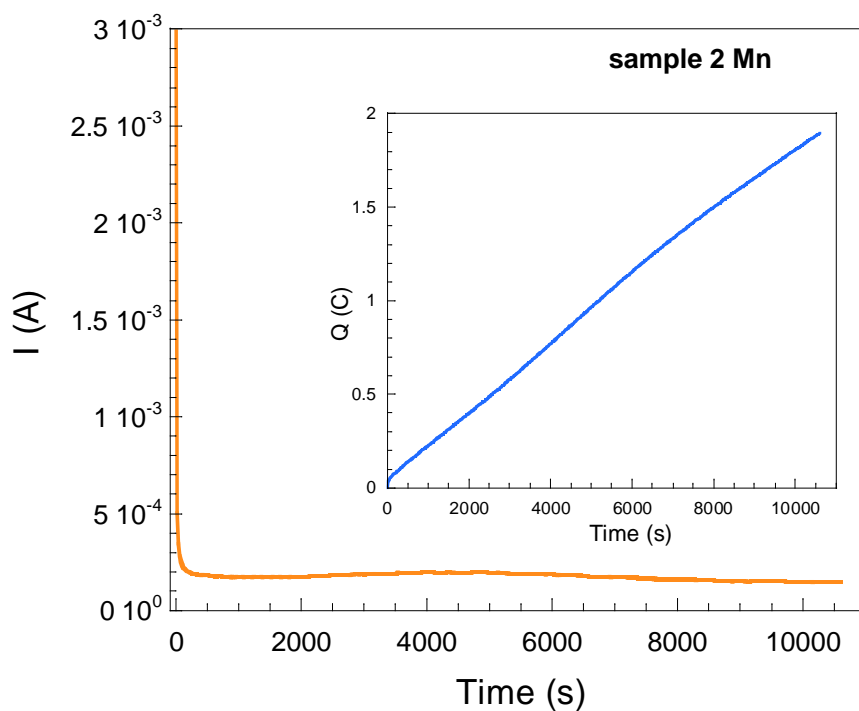


Fig 3A and 3B

After 0.35 C ( $t = 1770$  s), a peak at  $3.45^\circ$  ( $d_{\text{cal}} = 10.285 \text{ \AA}$ ) appears on diffractogram. According to the JCPDS card 32-1128, this peak could be attributed to the main pattern of busserite, which is a  $10 \text{ \AA}$  hydrous phyllomanganate [23]. After 1.0 C ( $t = 5225$  s), other peaks that can be also attributed to busserite, appear ( $6.85^\circ$ - $14.47^\circ$ ). The intensities of the peaks increase with time (or Q) and become very significantly at the end of synthesis principally for the main peak ( $3.51^\circ$ ). In contrary, the intensity of the main peak of  $\text{SnO}_2$  ( $10.61^\circ$ ) decreases due to the formation of a covering thin layer on substrate (estimated to  $2 \mu\text{m}$ ). At the end of synthesis, we obtained a very homogeneous and adherent black film, which looks like exactly at thin layers electrodeposited in a classical electrochemical cell.

Another synthesis was made in the same conditions, but with a focus on XRD measurements in the range  $2$ - $5^\circ$  for acquiring better signals (step:  $0.05^\circ$  -  $10$  s/step,  $600$  s for each scan), Fig. 4 (Sample 3).

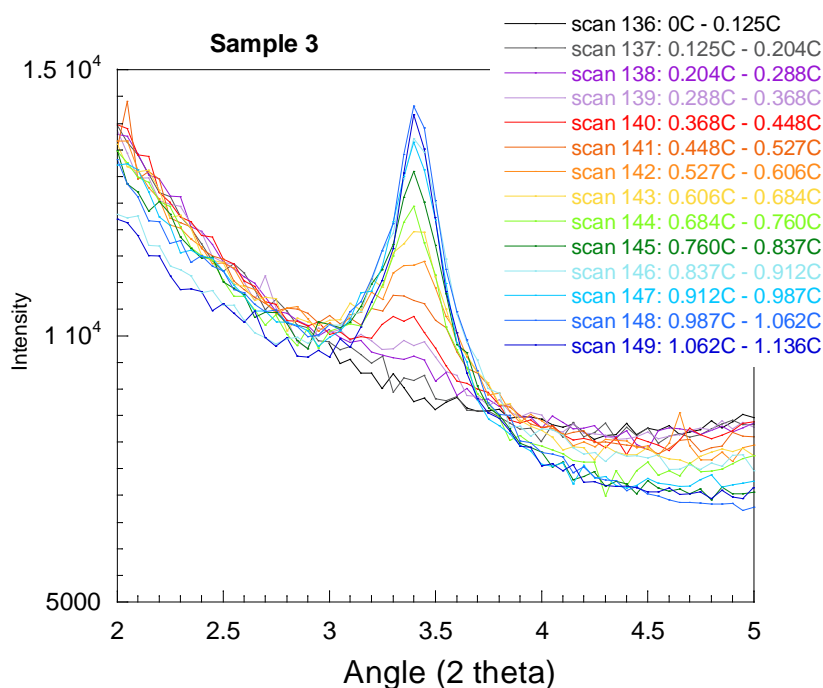
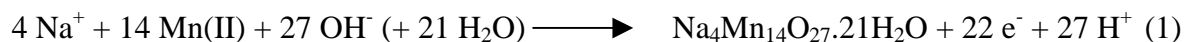


Fig. 4

All results are very reproducible: after 0.5 C, we observed always a significant peak characteristic of busserite ( $3.45^\circ$ - $d_{\text{cal}} = 10.285 \text{ \AA}$ ).

So, during the electrodeposition of thin layer of birnessite in aerated  $\text{Na}_2\text{SO}_4$  solutions at  $\text{pH}_{\text{initial}} = 5.3$ , the alone intermediary compound that is formed in-situ is busserite. According

to literature this compound is an unstable manganese oxide,  $\text{Na}_4\text{Mn}_{14}\text{O}_{27}\cdot 21\text{H}_2\text{O}$  that dehydrates to birnessite ( $\text{Na}_4\text{Mn}_{14}\text{O}_{27}\cdot 9\text{H}_2\text{O}$  or  $\text{Mn}_7\text{O}_{13}\cdot 5\text{H}_2\text{O}$ ) [22]. The electrochemical reaction in solution is reported below, Eq.1:



This compound was already identified as an intermediary compound during formation of birnessite in powder [24]. It is the first time that this compound was identified during electrodeposition of thin layer of birnessite, as far as we know.

### III – 3 Influence of $\text{pH}_{\text{initial}} = 4.2$

The thin layers of birnessite were electrodeposited in the same conditions ( $[\text{MnSO}_4] = 1.6 \cdot 10^{-3} \text{ M}$  in a  $\text{Na}_2\text{SO}_4$  0.4 M solution) but the  $\text{pH}_{\text{initial}}$  was adjusted at 4.2 (Sample 5). We chosen this value because it corresponds at the spontaneous value of the  $\text{pH}_{\text{final}}$  at the end of the “classical” synthesis ( $\text{pH}_{\text{initial}} = 5.3$ ) [20]. The final amount of electricity,  $Q_f$ , is equal to 2.40 C ( $t = 19040 \text{ s}$ ) and the value of  $\text{pH}_{\text{final}} = 4.09$ . During electrodeposition, systematic XRD measurements were recorded at constant times (2 – 32 °, step: 0.05 ° - 1 s/step, 600 s for each scan, Fig. 5A ; 2 – 27 °, step: 0.05 ° - 6 s/step, 3000 s for one scan, Fig. 5B).

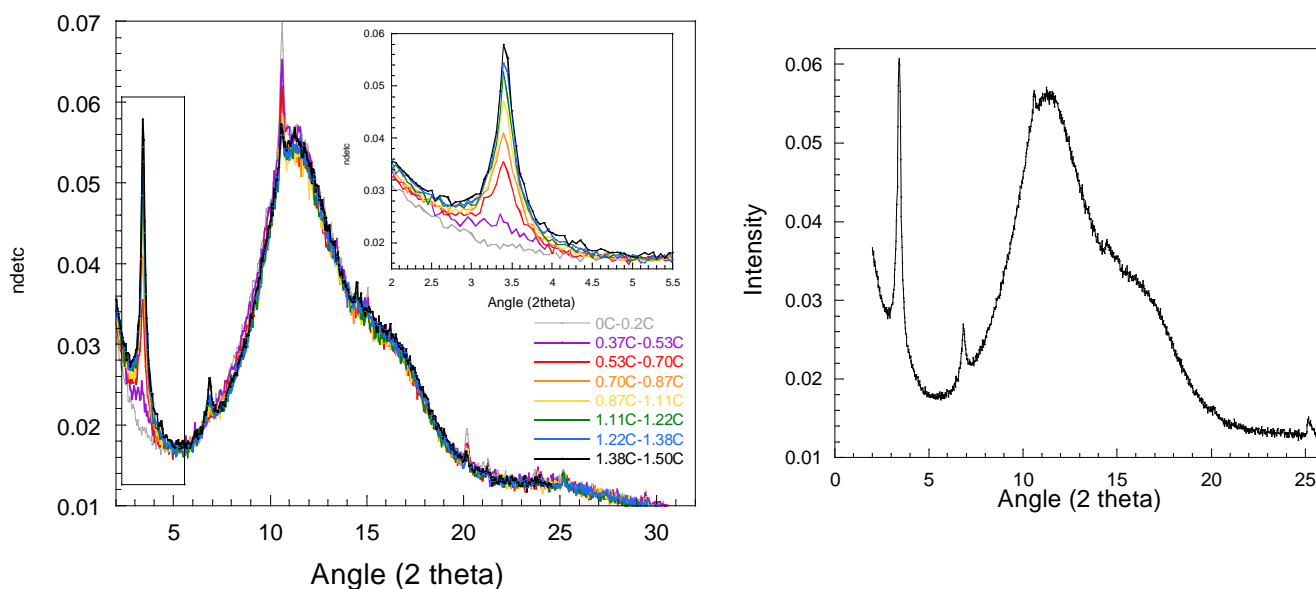


Fig. 5A and 5B

At pH = 4.2, busserite is also electrodeposited ( $3.41^\circ$  -  $d_{\text{cal}} = 10.405 \text{ \AA}$ ;  $6.83^\circ$ ), but the peak at  $14.5^\circ$  seems less defined. The peaks at  $10.58^\circ$  and  $25.16^\circ$  are attributed to substrate ( $\text{SnO}_2$ ). Others synthesis were done in the same conditions (sample 6:  $Q_f = 2.74 \text{ C}$  in 17260 s – sample 7:  $Q_f = 1.45 \text{ C}$  in 10380 s), and similar results are obtained (Fig. 6,  $2 - 18^\circ$ , step:  $0.05^\circ - 6 \text{ s/step}$ ), except on the peak at  $14.5^\circ$  (well defined for sample 6 – but one notes that the peak  $\text{SnO}_2$  is well defined also).

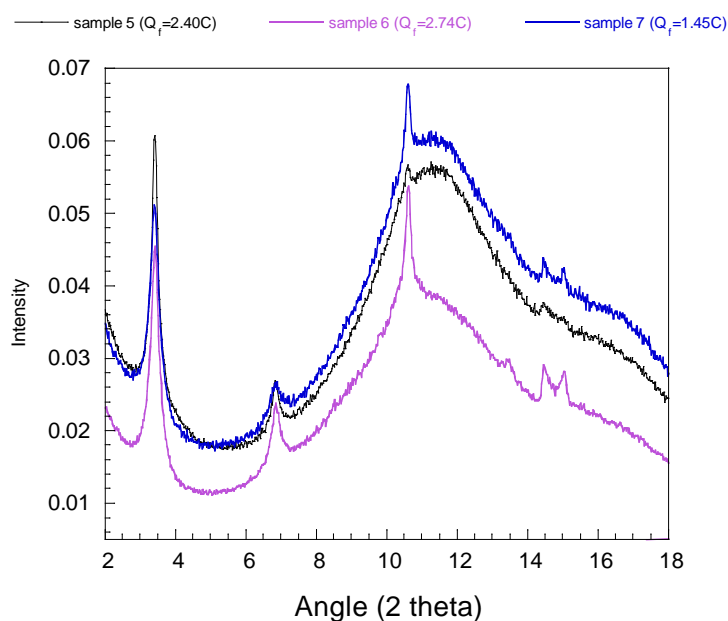


Fig.6

### III – 4 Conclusion on the influence of pH

During the electrodeposition of thin layer of birnessite in aerated  $\text{Na}_2\text{SO}_4$  solutions at  $\text{pH}_{\text{initial}} = 5.3$  or  $4.2$ , the alone intermediary compound that is formed in-situ is busserite with no significant difference on the position of peaks between these two values of pH, Fig.7.

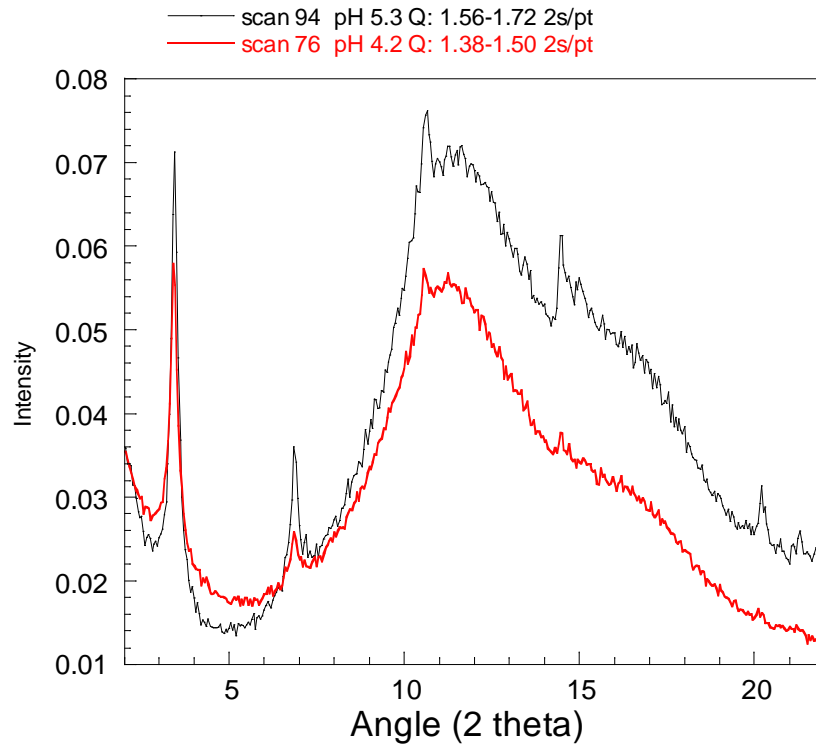


Fig 7

#### IV – Monitoring by XRD of dehydrate of busserite in real time.

So, during electrodeposition of thin layer of birnessite in aerated  $\text{Na}_2\text{SO}_4$  solutions, the alone intermediary compound that is formed in-situ is busserite. This compound is an unstable manganese oxide,  $\text{Na}_4\text{Mn}_{14}\text{O}_{27}\cdot 21\text{H}_2\text{O}$  that dehydrates to birnessite ( $\text{Na}_4\text{Mn}_{14}\text{O}_{27}\cdot 9\text{H}_2\text{O}$  or  $\text{Mn}_7\text{O}_{13}\cdot 5\text{H}_2\text{O}$ ) according to the literature, [22,24]

To verify this point, a same sample, which has been characterised previously in-situ, (sample 3) was characterised in the same cell but in the air after 48 hours, Fig. 8. The diffractogram obtained shows clearly characteristic peaks at  $4.88^\circ$ ,  $9.83^\circ$  and  $14.44^\circ$  ( $d = 7.272 \text{ \AA}$ ,  $3.614 \text{ \AA}$  and  $2.463 \text{ \AA}$  respectively), which could be attributed to  $\text{Mn}_7\text{O}_{13}\cdot 5\text{H}_2\text{O}$ , (JCPDS card 23-1239:  $4.92^\circ$ ,  $9.83^\circ$ ,  $14.46^\circ$ ) rather than Na-birnessite (JCPDS card 23-1046:  $5.00^\circ$ ,  $9.97^\circ$ ,  $14.17^\circ$  and  $14.70^\circ$ ). This result seems in good agreement with Lanson et al. who reported equivalent experimental valued of  $d$  at  $\text{pH}=5$  ( $7.265 \text{ \AA}$ ,  $3.614 \text{ \AA}$ ,  $2.466 \text{ \AA}$ ), and which suggested the transformation of Na-Busserite into H-Birnessite at this pH. [22].

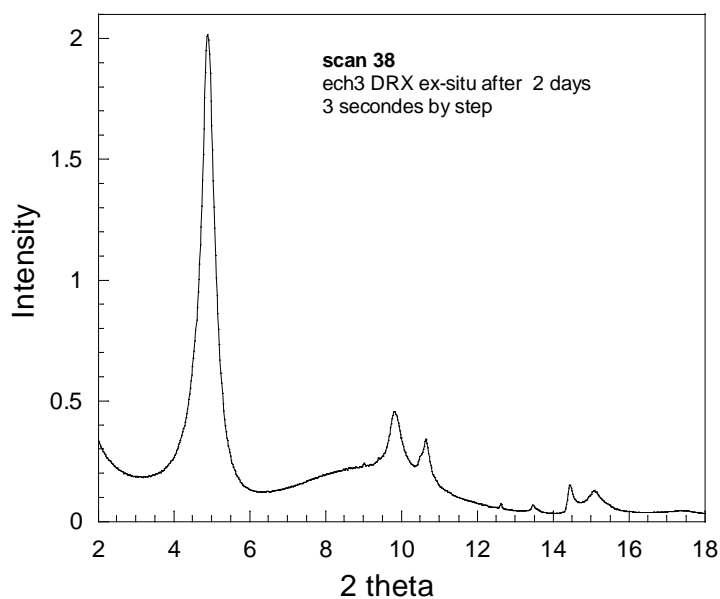


Fig. 8

So, after two days, the totality of busserite was transformed into birnessite. But, it was interesting to evaluate the time took for dehydration of busserite into birnessite. For that, we synthesised a thin layer of busserite, and after rinse (10 mn with milli-Q water), the cell has been not emptied but the film of kapton was removed to put progressively the thin layer in contact with the air (sample 10). During this step, systematic XRD measurements were recorded at constant times (2 – 22 °, step: 0.05 ° - 2 s/step, 800 s for each scan); only some scans are represented on Fig. 9 A.

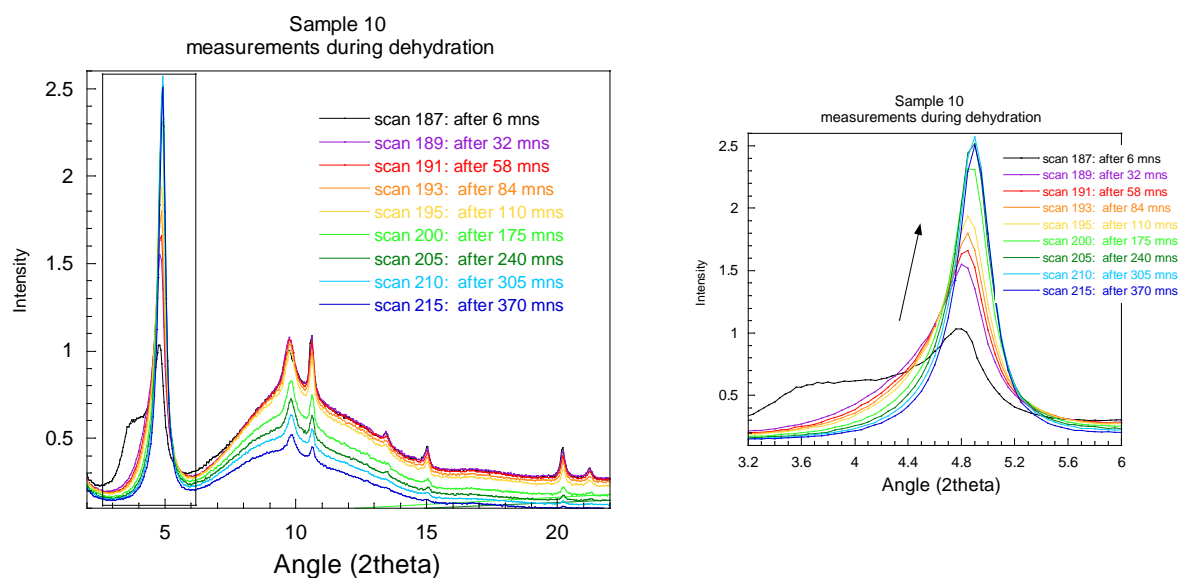
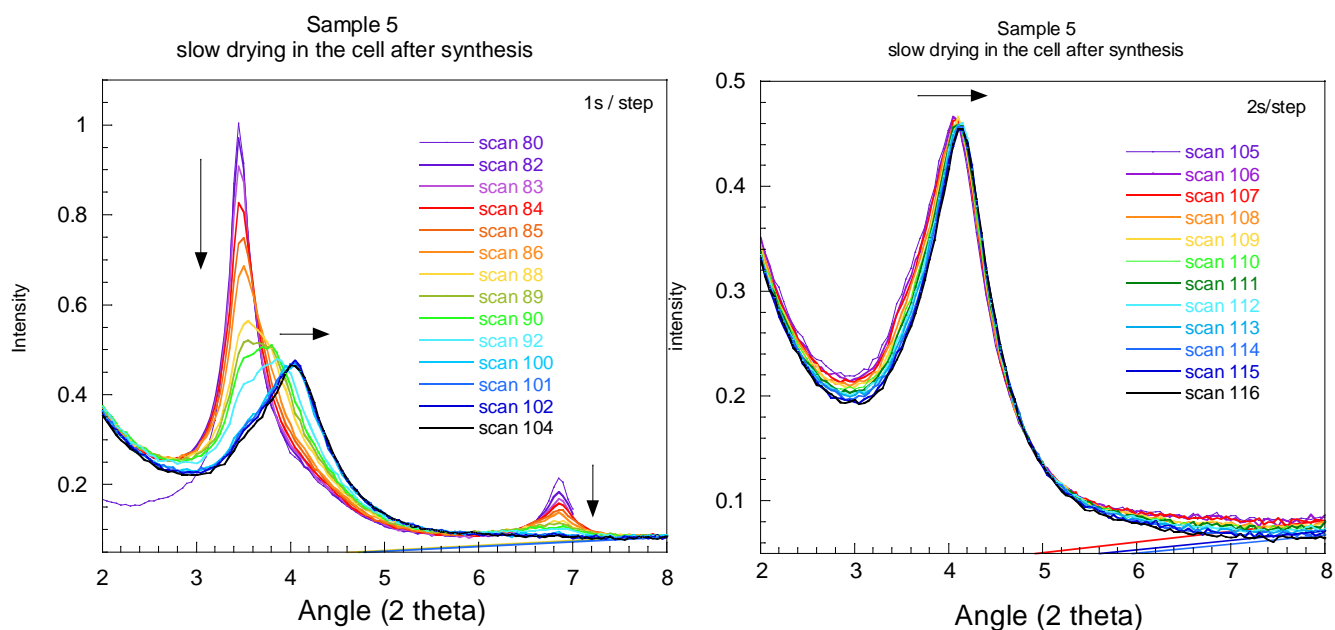


Fig 9A and 9B

We had some problem in the beginning of this experiment for acquiring XRD measurements but we can still conclude that the dehydration of busserite into birnessite is relatively fast, because after only five minutes, the two compounds are present. In fact, the characteristic peak of birnessite appears ( $4.79^\circ$  and  $9.79^\circ$ ) and only a shoulder corresponding to busserite is visible (scan 187). Moreover, reaction is total after only around twenty minutes. We observed with time a slight shift of the main peak of birnessite from  $4.79^\circ$  to  $4.90^\circ$ , corresponding to  $d = 7.409 \text{ \AA}$  to  $7.243 \text{ \AA}$  respectively.

To improve the studying of the transition of busserite into birnessite for quick times, we tried to dehydrate more slowly the sample (Sample 5). For that, it was dehydrated inside the cell with a flux of air send by the micropump during around 6 hours (Sine, 20 Hz,  $V = 250 \text{ Vpp}$ ), after a rinse with milli-Q water during ten minutes. During this step, systematic XRD measurements were recorded at constant times in various conditions (Fig. 10A:  $2 - 7^\circ$ , step:  $0.05^\circ - 1 \text{ s/step}$ , 100 s for each scan (scan 78-scan 104); Fig. 10B:  $2 - 7^\circ$ , step:  $0.05^\circ - 2 \text{ s/step}$ , 200 s for each scan (scan 105-scan 116); Fig. 10C:  $2 - 7^\circ$ , step:  $0.05^\circ - 4 \text{ s/step}$ , 600 s for each scan (scan 122-scan 131); Fig. 10D:  $2 - 7^\circ$ , step:  $0.05^\circ - 6 \text{ s/step}$ , 600 s for each scan (scan 122-scan 131); ); Fig. 10E:  $2 - 27^\circ$ , step:  $0.05^\circ - 6 \text{ s/step}$ , 3000 s for each scan (scan 138)).



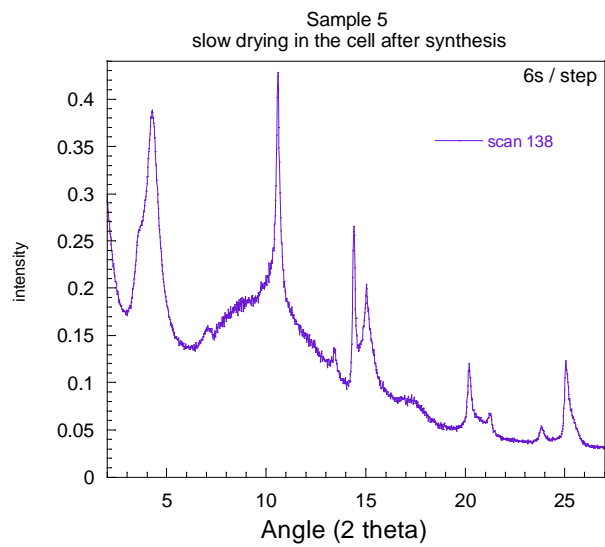
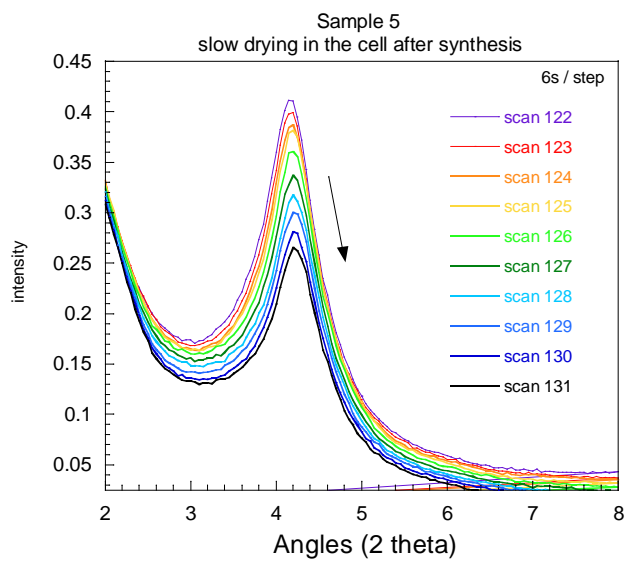
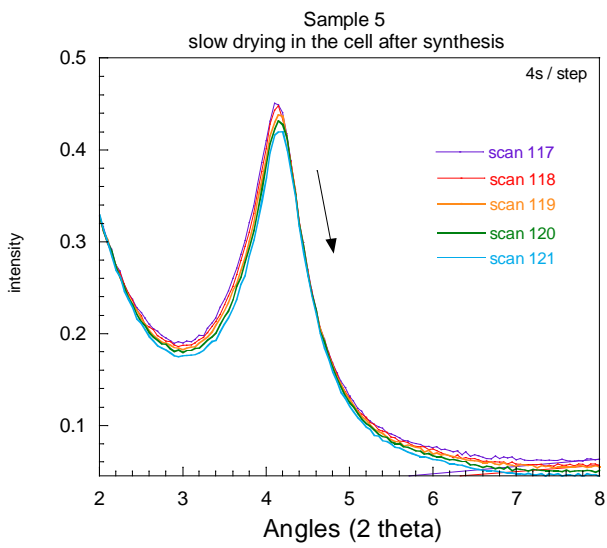


Fig 10A -10E

In a first time (Fig 10A), the intensity of the main peak of busserite ( $3.45^\circ$ ) and the second peak situated at  $6.85^\circ$  decreases with time, and for this latter disappears totally after around 1000 s (scan 80 to scan 88). This value of time corresponds also to the enlargement and shift of the main peak of busserite from  $3.45^\circ$  to  $4.03^\circ$  ( $d = 10.285 \text{ \AA}$  to  $d = 8.805 \text{ \AA}$  respectively). After this step, only a slight shift of this main peak from  $4.03^\circ$  to  $4.23^\circ$  ( $d = 8.805 \text{ \AA}$  to  $8.634 \text{ \AA}$ ), was observed, with a very small decrease of the intensity.

On the last scan registered after six hours with a better precision, Fig 10E, we can note that the main peak at  $4.28^\circ$  ( $d = 8.291 \text{ \AA}$ ) is not situated to the value of the characteristic peak of birnessite ( $4.90^\circ$ ,  $d = 7.243 \text{ \AA}$ ) or busserite. It could correspond to a compound presenting an intermediary structure. This hypothesis is reinforced by the presence of others peaks characteristic of these two compounds, except  $\text{SnO}_2$  peaks ( $10.61^\circ$ ,  $13.44^\circ$ ,  $15.04^\circ$ ,  $20.19^\circ$ ,  $21.2^\circ$ ,  $23.81^\circ$ ,  $25.055^\circ$ ). In fact, a shoulder around  $3.65^\circ$  and the small peak situated at  $7.07^\circ$  could be attributed to Na-busserite. The significant peak at  $14.40^\circ$  could be attributed to Na-busserite and birnessite, and the shoulder at  $17.41^\circ$  could be attributed to birnessite.

Some publications report that dehydration busserite/birnessite could be reversible. To verify this point, milli-Q water was reintroduced inside the cell with the micropump (Sine, 20 Hz,  $V = 250 \text{ Vpp}$ ). The XRD measurements presented on Fig. 11 show no significant change of the position of the peak ( $4.30^\circ$ ). Moreover, the intensity stays very weak.

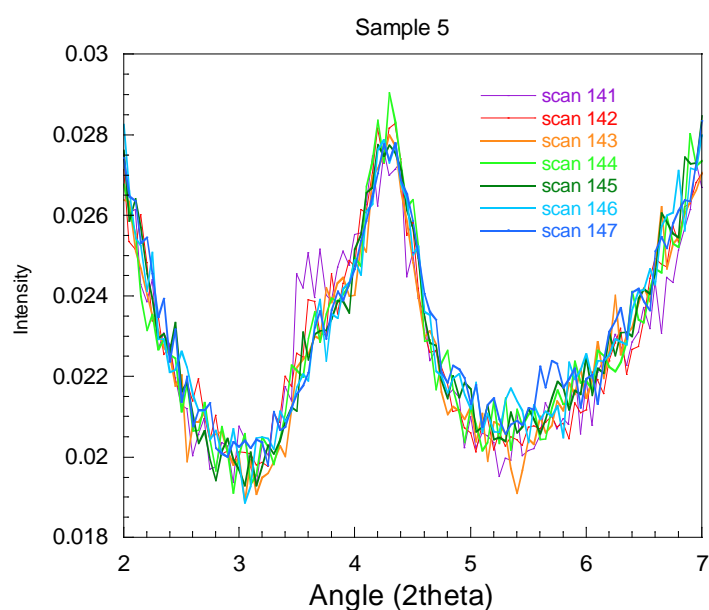


Fig. 11

## V – Electrodeposition of thin layers of birnessite in presence of $K^+$ .

It was interesting to study the influence of cation on the nature of intermediary compound during electrodeposition. For that, thin layers of birnessite were electrodeposited in the same conditions ( $[MnSO_4] = 1.6 \cdot 10^{-3} \text{ M}$ ,  $pH_{\text{initial}} = 5.30$ ) but in a  $K_2SO_4$  0.4 M (Sample 8). The final amount of electricity,  $Q_f$ , is equal to 2.60 C in 15360 s. Before the electrodeposition, the cell, the reference electrode, the micropump and pipes were rinsed during 10 mn with milli-Q water, and after 10 mn with  $K_2SO_4$  solution (0.4 M). Moreover, a new film of kapton was used to avoid problems of pollution.

During electrodeposition, systematic XRD measurements were recorded at constant times. No significant peak was visible during electrodeposition even for  $Q$  superior at 1.40 C, that is why only the final scan was presented on Fig. 12A ( $2 - 27^\circ$ , step:  $0.05^\circ - 6 \text{ s/step}$ ). At the end of the synthesis in a solution of  $K_2SO_4$ , only two peaks are visible in addition to those of the substrate, the first one around  $4.79^\circ$  (very broad), and the second one at  $14.51^\circ$  (well defined), which could be attributed to birnessite ( $Mn_7O_{13} \cdot 5H_2O$ ).

An ex-situ diffractogram was also recorded in the air on the very homogeneous black thin layer, Fig. 12B. The main peak was shifted from  $4.79^\circ$  to  $4.88^\circ$  with an important increasing of intensity (expected due to the difference of medium: aqueous solution/air). Two new peaks appear at  $9.80^\circ$  and  $14.66^\circ$ , which can be also attributed to birnessite,  $Mn_7O_{13} \cdot 5H_2O$  (JCPDS card 23-1239).

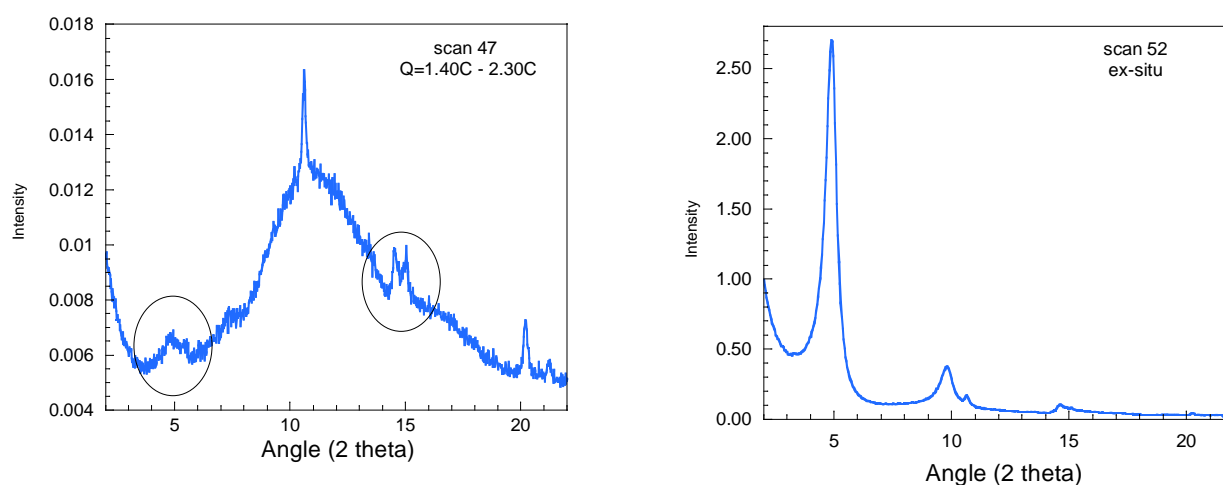


Fig. 12A (in-situ) and B (ex-situ)

We can note that the peaks of SnO<sub>2</sub> are quasi disappeared due to a very covering thin layer.

In conclusion, during the electrodeposition of thin layer of birnessite in aerated K<sub>2</sub>SO<sub>4</sub> solutions at pH<sub>initial</sub> = 5.3, the alone compound that is formed in-situ is birnessite. Others syntheses were made (Sample 9 at 50 °C; sample 11 at 25°C), and similar results were obtained. This result could be due to a difference of hydration between Na<sup>+</sup> and K<sup>+</sup> cation.

## VI – Behaviour of thin layers of buserite.

### VI – 2 Reduction of thin layer in a MnSO<sub>4</sub> solution

It was interesting to study the redox behaviour of thin layer of buserite. For that, just after synthesis, a reducing potential, chosen according to a cyclic voltamperometric study made previously in our laboratory, was applied on the thin layer (E = -0.15 V) (sample 6, Q<sub>f</sub> = 2.74 C, t = 17260 s) in the same solution that used for synthesis (MnSO<sub>4</sub> - Na<sub>2</sub>SO<sub>4</sub>; V = 272 mL, pH = 4.10) but in re-circulation with micropump (Sine, 20 Hz, V = 250 Vpp). During reduction, systematic XRD measurements were recorded at constant times. Only the last scan was presented on Fig. 13 (6 s/step) and compared with diffractogram obtained during electrodeposition.

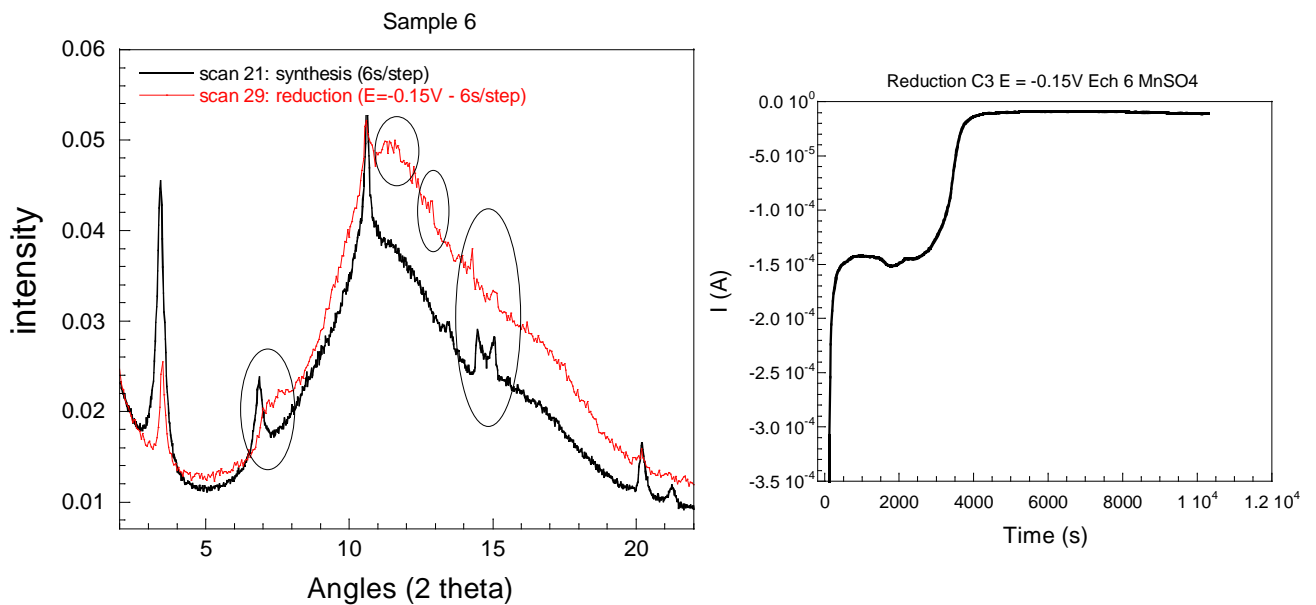


Fig. 13A and 13B

Some changes were observed after reduction at  $E = -0.15$  V (scan 29:  $Q_{\text{reduction}} = -0.722$  C to  $-0.815$  C): the decrease of intensity of the main peak of busserite with a slight shift ( $3.44^\circ$  to  $3.50^\circ$ ), the shift of the busserite peak at  $14.46^\circ$  to  $14.30^\circ$ , which could be attributed to hausmannite ( $\text{Mn}_3\text{O}_4$ , card JCPDS 24-734), a shoulder at  $11.5^\circ$  (which could be attributed also to hausmannite), and a shoulder around  $7.0 - 8.0^\circ$ .

An ex-situ characterisation in the air was made on sample after rinse with milli-Q water during ten minutes, Fig. 14.

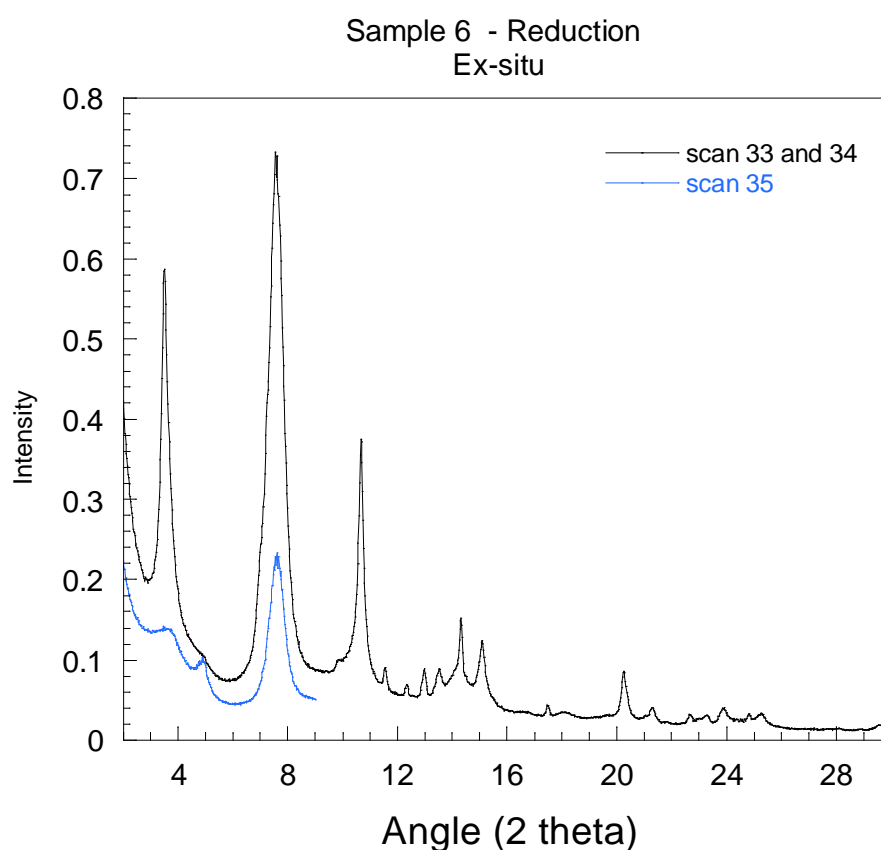


Fig 14

Significant peaks are visible on diffractogram. In addition of busserite, hausmannite ( $\text{Mn}_3\text{O}_4$ ) is highlighted due to the characteristic peaks situated at  $11.52^\circ$ ,  $12.97^\circ$  and  $14.31^\circ$ , and feitknechtite ( $\beta\text{-MnOOH}$ , JCPDS card 18-804) with peaks at  $7.60^\circ$ ,  $13.54^\circ$  and  $18.12^\circ$  ( $\text{SnO}_2$ :  $10.63^\circ$ ,  $15.07^\circ$ ,  $20.20^\circ$ ,  $21.32^\circ$ ,  $23.91^\circ$  and  $25.28^\circ$ ). After some minutes (around 33 minutes which correspond to the beginning of scan 35), a characteristic peak of birnessite is visible at  $4.91^\circ$  with a small intensity compared to a simple dehydration (see sample 10, Fig. 9). This result could be due to the presence of hausmannite and/or feitknechtite on the

surface, which can block the dehydration of thin layer of busserite. It appears normal that birnessite is always present because the  $Q_{f \text{ reduction}} < Q_{f \text{ synthesis}}$ . At the end of this experiment, the sample, which stays adherent and homogeneous, seems browner than after synthesis in good agreement with the presence of Mn(III) compounds.

### VI – 3 Reduction of thin layer in a $\text{Na}_2\text{SO}_4$ solution in absence of Mn(II) ions

It was interesting to study the potential role of Mn(II) ions during redox behaviour of thin layer of busserite. For that, just after synthesis, the sample was rinsed with milli-Q water during ten minutes and a solution of  $\text{Na}_2\text{SO}_4$  0.4 M also during ten minutes.

After, a known volume of a  $\text{Na}_2\text{SO}_4$  0.4 M solution, with the same parameters than previous experiment ( $V = 272$  mL,  $\text{pH} = 4.10$ ) was re-circulated inside the electrochemical cell with the micropump (Sine, 20 Hz,  $V = 250$  Vpp). The same value of reducing potential, ( $E = -0.15$  V) was applied on the thin layer (sample 7, 02/10/09,  $Q_f = 1.45$  C,  $t = 10380$  s. During reduction ( $Q_f = -0.681$  C,  $t = 23772$  s), systematic XRD measurements were recorded at constant times. Only some scans are presented on Fig. 15 (2 s/step).

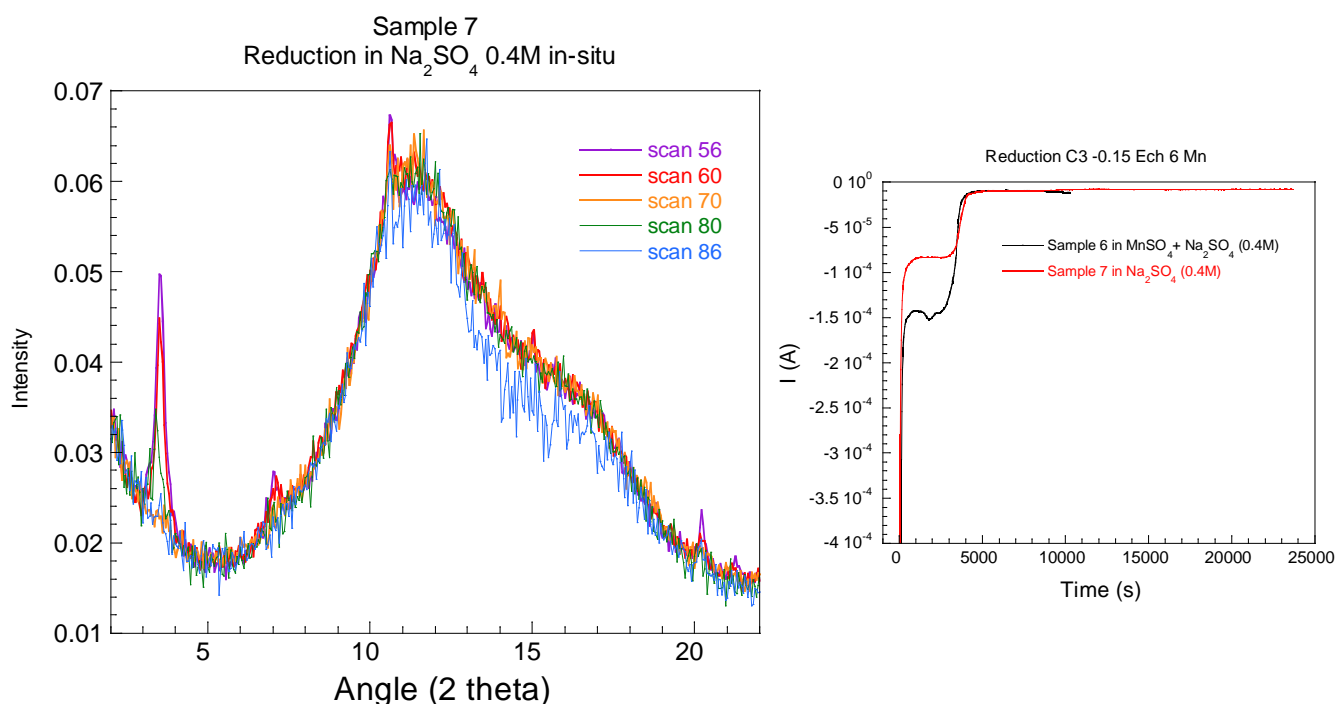


Fig 15

According in-situ measurements, we observed only a decrease of the intensity of the buserite peaks. No other peak of crystallised compound was observed. Moreover, a great decrease of the signal (95 %) was noted. After rinse with milli-Q water during 10 min, the electrochemical cell was opened and we can see that 80 % of the thin layer was removed. However, we can still analyse the solid by ex-situ XRD measurements, Fig. 16.

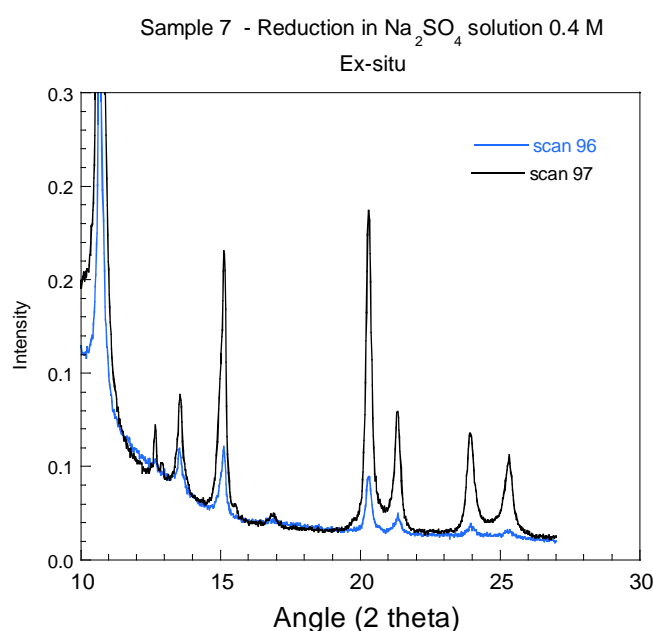


Fig 16

In these conditions of reduction, buserite (3.58 °), birnessite (4.91 °, 9.91 ° (shoulder)), and feitknechtite ( $\beta$ -MnOOH, 7.66 °) are identified. It appears normal that buserite or birnessite are always present because the  $Q_{f \text{ reduction}} < Q_{f \text{ synthesis}}$ . In opposite of the previous reduction, hausmannite (Mn<sub>3</sub>O<sub>4</sub>) is not present. So, we can suppose that this latter compound can be formed during reduction only if Mn(II) ions are present in the solution. The fact that the solid was dissolved could be due to the absence of hausmannite that could block the surface, as previously. But this point must be confirmed with other experiments before conclude.

#### VI – 4 Behaviour of the thin layer towards the solution of MnSO<sub>4</sub> after synthesis

We wanted to know if the presence of Mn(II) ions in solution could induce an anti-dismutation reaction like:



Some samples (2,3) stayed in contact with MnSO<sub>4</sub> solution after synthesis. It is difficult to conclude on XRD measurements if others compounds were formed due to an anti-dismutation reaction. These experiments must be completed.

## VII – Conclusion and perspectives

For the first time, the intermediary compound was determined during the electrodeposition of thin layer of birnessite on SnO<sub>2</sub> in function of medium. In aerated Na<sub>2</sub>SO<sub>4</sub> solution, and independently of pH<sub>ini</sub> (5.3 or 4.2), busserite is electrodeposited as an in-situ intermediary compound. We have shown that the dehydration of busserite into birnessite is relatively rapid and takes less than 30 minutes if the thin layer is in the air. In aerated K<sub>2</sub>SO<sub>4</sub> medium, birnessite is directly electrodeposited.

We have shown also that our electrochemical cell can be used to study the redox behaviour of thin layer in various conditions. If the reduction is done in presence of Mn(II) ions, feitknechtite and hausmanite are formed on the surface and the thin layer is blocked. In contrary, the reduction in absence of Mn(II) ions leads only to feitknechtite, with dissolution of thin layer. The fact that the solid was dissolved could be due to the absence of hausmannite that could block the surface. But this point must be confirmed with other experiments before conclude.

These first experiments are very interesting and encouraging. This special electrochemical cell appears as a successful tool for characterising compounds during electrochemical measurements (electrodeposition, redox behaviour,...). It will be interesting to improve this cell for measurements in absence of oxygen. Indeed, the presence or the absence of oxygen modifies significantly mechanisms, as we reported during electrodeposition of thin layers of birnessite previously [20]. In future, numerous perspectives with iron compounds (siderite) and manganese compounds in interaction with various pollutants (dyes, pesticides, radioelement,...) can be studied.

## References

- [1] J. E. Post, Proc. Natl. Acad. Sci. **96**, 3447 (1999).
- [2] D. Frias et al., Mater. Charact. **58**, 776 (2007)
- [3] A.C. Gaillot, PhD Thesis, University of Grenoble (2002).
- [4] X.H. Feng et al., Environ. Poll. **147**, 366 (2007).
- [5] M.J. Scott et al., Environ. Sci. Technol. **30**, 1990 (1996).
- [6] A. Manceau, et al., J. Colloid Interface Sci. **148**, 425 (1992).
- [7] P.M. Huang, in: D.L. Sparks & D.L. Suarez (Eds) Soils Sci. Soc. Am. Madison, WI, p 191-230 (1992).
- [8] R. Han, et al., J. Environ. Radioact. **93**, 127 (2007).
- [9] L. Al-Attar, et al., J. Mater. Chem. **12**, 1381 (2002).
- [10] C-H. Wu, C-L. Chang, J. Hazard. Mat. **B128**, 265 (2006).
- [11] L. Mao et al, Electrochim. Acta **49**, 2515 (2004).
- [12] E. Macheaux et al., J. Pow. Sources **157**, 443 (2006).
- [13] V. Subramanian et al., J. Pow. Sources **159**, 361 (2006).
- [14] J.P. Viricelle et al., Mater. Sci. Eng. **C 26**, 186 (2006).
- [15] J. Eikenberg et al., J. Environ. Radioact. **54**, 109 (2001).
- [16] M. Nakayama et al., Chem. Lett. **33**, 670 (2004).
- [17] Y.K. Zhou et al., J. Phys. Chem. Solids **67**, 1351 (2006).
- [18] S. Peulon et al. J. Electrochem. Soc., 145(3), (1998), 864-874.
- [19] S. Peulon et al., Electrochim. Acta **52**, 7681 (2007).
- [20] N. Larabi-Gruet et al., Electrochim. Acta **53**, 7281 (2008).
- [21] V. A. Drits, E. Silvester, A. I. Gorshkov, A. Manceau, American Mineralogist, 82 (1997) 946.
- [22] B. Lanson, V. A. Drits, E. Silvester, A. Manceau, American Mineralogist, 85 (2000) 826.
- [23] R. Burns et al. American Mineralogist, **68**, 972 (1983).
- [24] X. Feng et al. Science in China Ser. D Earth Sciences, 48, 1438 (2005).